Published in final edited form as:
J Biomech. 2014 June 27; 47(9): 2006–2012. doi:10.1016/j.jbiomech.2013.11.003.

Dynamic Contact Mechanics on the Tibial Plateau of the Human Knee During Activities of Daily Living

Susannah Gilbert[*], **Tony Chen**[*], **Ian D. Hutchinson**, **Dan Choi**, **Clifford Voigt**, **Russell F. Warren**, and **Suzanne A. Maher**
Hospital for Special Surgery, 535 East 70th Street, New York, NY 10021, United States

Abstract

Despite significant advances in scaffold design, manufacture, and development, it remains unclear what forces these scaffolds must withstand when implanted into the heavily loaded environment of the knee joint. The objective of this study was to fully quantify the dynamic contact mechanics across the tibial plateau of the human knee joint during gait and stair climbing. Our model consisted of a modified Stanmore knee simulator (to apply multi-directional dynamic forces), a two-camera motion capture system (to record joint kinematics), an electronic sensor (to record contact stresses on the tibial plateau), and a suite of post-processing algorithms. During gait, peak contact stresses on the medial plateau occurred in areas of cartilage-cartilage contact; while during stair climb, peak contact stresses were located in the posterior aspect of the plateau, under the meniscus. On the lateral plateau, during gait and in early stair-climb, peak contact stresses occurred under the meniscus, while in late stair-climb, peak contact stresses were experienced in the zone of cartilage-cartilage contact. At 45% of the gait cycle, and 20% and 48% of the stair-climb cycle, peak stresses were simultaneously experienced on both the medial and lateral compartment, suggesting that these phases of loading warrant particular consideration in any simulation intended to evaluate scaffold performance. Our study suggests that in order to design a scaffold capable of restoring ‘normal’ contact mechanics to the injured knees, the mechanics of the intended site of implantation should be taken into account in any pre-clinical testing regime.

Introduction

The human knee experiences complex multidirectional and dynamically varying forces during activities of daily living. Technologies intended to repair or replace damaged joint tissue must not only withstand these complex forces but should also carry and distribute loads much in the way of the native tissue. Despite significant advances in scaffold design,

Address for Correspondence: Suzanne A. Maher, PhD, Associate Scientist, Hospital for Special Surgery, 535 East 70th Street, New York, NY 10021, Ph: 212.606.1083, Fax: 212.249.2373, mahers@hss.edu.
[*]Shared first authorship

Conflict of interest statement:
None of the authors have conflicts that relate to the content of this manuscript.

manufacture and development (AufderHeide and Athanasiou, 2004; Freed et al., 2006), it remains unclear what forces these scaffolds are likely to be subjected to *in vivo*. This deficit in knowledge is caused in part by the absence of a model that can allow for the direct measurement of knee joint contact mechanics under physiological loads that represent activities of daily living.

Instrumented total knee replacements have been used to record the forces acting on patients' prostheses during everyday activities, but the regional distribution of contact forces or the effect of soft tissue injury and repair on those forces cannot be assessed. *In vivo* gait analysis studies have quantified how the tibia moves relative to the femur during walking (Dyrby and Andriacchi, 2004; Scanlan et al., 2010), but the resulting contact mechanics cannot be directly measured. Computational models can be programmed to apply complex multidirectional loading conditions across *in silica* representations of the knee joint (Hopkins et al., 2010; Netravali et al., 2011) that capture the anisotropy and inhomogeneity of the soft tissues (Mononen et al., 2013), but the challenges of creating and experimentally validating the data generated have not yet been met. Cadaveric studies have been used to physically measure the contact forces across the knee joint using electronic sensors (Mundermann et al., 2008; Taylor et al., 1997) and pressure-sensitive film (Fornalski et al., 2012; Seitz et al., 2012); but the models typically apply static (Seitz et al., 2012), or quasi-static loads (Li et al., 2004; Wunschel et al., 2012) and oftentimes the applied forces are a fraction of that expected *in vivo* (Li et al., 2004; Wunschel et al., 2012). In models that capture the multidirectional nature of loading during simulated activities of daily living (Bedi et al., 2010), analysis of contact mechanics has been restricted to pre-defined points within the gait cycle, thus a full analysis of dynamic contact mechanics throughout any activity is not yet available. The objective of this study was to fully quantify the dynamic contact mechanics across the tibial plateau of the human knee joint throughout experimentally simulated activities of gait and stair climbing.

Methods

The fixtures of a Stanmore knee simulator were modified to accept a cadaveric knee. 5 fresh frozen cadaveric knees, midshaft femur to midshaft tibia, (3 Female, 2 Male, ages 39–62) were prepared as previously described (Bedi et al., 2010), Figure 1. The inputs to simulate gait were obtained from ISO standard #14243-1 (Taylor et al., 1997) while stair climb data was input from a study by Fantozzi et al., 2003, Figure 2. To accommodate the maximum flexion angle of 65° possible with the simulator, the stair ascent flexion input was modified to exclude 0–20% and 75–100% of the cycle during which time axial loads are relatively low, but flexion angles of up to 120° occur.

A polycarbonate reference marker (Fiducial) consisting of pre-machined lines was fixed on the proximal tibia. The Fiducial and the 3D location of tibial landmarks (insertion of the collateral ligaments and a point most distal to the joint line) were traced with a 3D microscribe digitizer (Reware, Raleigh, NC). A 2-camera motion capture system (Motion Analysis, Santa Rosa, CA) was used to capture the 3D positions of the femur, tibia and a pointer (used to digitize femoral landmarks) at 50 Hz throughout gait and stair-climb. These landmarks were then used to quantify knee motion with custom software developed in

MATLAB (Mathworks, Naticl, MA) using a variant of (Grood and Suntay, 1983). In our definition, the transepicondylar axis is preserved as the flexion axis while the malleoli midpoint is replaced with a point on the tibia that is most distal to the joint line, to define tibial axis rotation. The varus-valgus axis remains as the floating axis derived from the other two axes, and the translations are defined as the motion of the tibial center (collateral insertion midpoint) relative to the femoral center (epicondylar midpoint). An assessment of the effect of this modified approach on computed joint kinematics is outlined in Supplement A.

An electronic sensor (4010N, Tekscan, MA) composed of a matrix of 22×34 sensing elements (sensels: each measuring 1×1mm and separated from its neighboring sensel by 0.5 mm), capable of quantifying the contact stress normal to its surface (100 Hz), hereafter called ‘contact stress’, was used. Each sensor was augmented with plastic tabs and a layer of Durapore™ surgical tape (3M, MN), sealed between two layers of Tegaderm™ adhesive dressing (3M, MN), calibrated and equilibrated (Brimacombe et al., 2009). Once inserted under the menisci, the sensor was fixed to the surface of the medial and lateral tibial plateau by suturing the plastic tabs to the posterior knee capsule and close to the tibial insertion of the anterior cruciate ligament.

The position of the femur-tibia complex under 1000 N of axial force (used to represent the neutral position of the knee during stance), as recorded by the camera-based system, was used as a reference from which all translations and rotations were calculated. The simulator was programmed to apply 20 cycles of gait (at 0.5 Hz) and stair ascent (at 0.25 Hz).

Using custom MATLAB code, the following contact parameters were computed for each frame of data recorded for the medial and lateral compartments: (i) contact area, (ii) maximum contact stress, and (iii) total load. For each knee, two regions of interest (ROI) were selected based on the contour stress maps that occurred at 14% of the gait cycle, representing cartilage-cartilage and meniscal-cartilage contact. Gaussian distributions of load were identified as the cartilage-cartilage contact region and the remaining loaded sensels on the plateau were taken as the cartilage-meniscal contact area. The ROIs were identified 3 independent times and the area of contact and load carried by each region was computed throughout loading.

Based on prior studies that have indicated a relationship between velocity of tibial-femoral contact and rate of cartilage degeneration (Beveridge et al., 2013), and a relationship between shear stress magnitude and structural organization of cell-seeded scaffolds for articular cartilage defects (Chen et al., 2012), we sought to describe the movement of contact on the tibia. The (X, Y) location of the weighted center of contact ($WCoC_X$, $WCoC_Y$) for the medial and lateral plateau for each frame of data throughout the gait cycle were computed (see Supplement B & Gee and Wang et al., in review), where X is in the medial-lateral direction and Y is in the anterior-posterior direction. The instantaneous anterior/posterior (AP) velocities as well as the internal/external (IE) velocities for the WCoC were computed.

Results

Knee kinematics followed well defined and reproducible patterns (Figure 3A&B), with minimal medial-lateral translations (5–7mm) and varus-valgus rotations (3–7°) in gait and stair climb. The area of contact across the medial and lateral plateau was lowest immediately after heel strike, but after about 15% of the gait cycle remained relatively constant until about 40% of the gait cycle (Figure 4A). On the medial plateau, maximum contact stresses occurred at 5% and 45% of the gait cycle (4.38 ± 0.62 MPa and 5.61 ± 1.53 MPa, respectively: Figure 4B) and were located in the area of cartilage-cartilage contact. On the lateral plateau, the maximum contact stress occurred at 14% and 45% of the gait cycle with average values of 7.26 ± 2.51 MPa and 5.65 ± 3.14 MPa respectively (Figure 4B). At 14% of the gait cycle, the average maximum stress on the medial plateau was 3-fold lower than the maximum stress on the lateral plateau. However, when the total load carried by the plateaus was computed, equal load was carried on the medial and lateral plateaus throughout early stance (Figure 4C).

During stair climbing, the area of contact on the medial and lateral plateaus were similar except between 45% and 60% of the cycle (Figure 4D), where higher areas of contact were seen on the lateral plateau. Peak stresses on the medial plateau were located on the posterior aspect, under the meniscus, with values of 7.73 ± 2.92 MPa and 4.41 ± 2.17 MPa respectively at 20% and 48% of the cycle (Figure 4E). Peak stresses on the lateral plateau remained in the area of meniscal contact at 20% of the cycle (7.43 ± 2.32 MPa), but moved to the zone of cartilage-cartilage contact at 48% of the cycle (3.05 ± 0.52 MPa), respectively (Figure 4E). Total load was shared equally between the plateaus during stance phase (Figure 4F).

The cartilage-cartilage contact ROI (Figure 5A) and meniscal-cartilage contact ROI (Figure 5B) were used to calculate the area ratios (Figure 5C) and load ratios (Figure 5D) for the medial and lateral plateau. For gait, consider the medial plateau contact area ratio: higher contact area occurred under the meniscus than under the zone of cartilage-cartilage contact throughout gait, with the exception of terminal stance (approximately 60% of the gait cycle), when the contact area in the cartilage-cartilage zone was higher than that under the meniscus. The load ratio data, demonstrated that cartilage under the meniscus carried a higher proportion of the load, than the area of cartilage-cartilage contact at around 15–25% of the gait cycle, while for the remainder of the cycle, load was predominantly born by the cartilage-cartilage zone. Data from the lateral plateau, suggested that area of contact was consistently higher under the meniscus for the entirety of the gait cycle, while higher stresses were born by the cartilage under the meniscus throughout gait.

The same regions of interest outlined for gait were used for stair climbing (Figure 5E and F) and were used to calculate the contact area ratio (Figure 5G) and load ratio (Figure 5H) throughout stair climb. Higher contact area was present under the meniscus than under the zone of cartilage-cartilage contact throughout stair-climb for both compartments. The load ratio data further suggested that a higher proportion of the load was carried by the meniscus on the medial and lateral plateau, except on the lateral plateau during 40% to 50% of stair-climb, when a higher proportion of load was carried in the cartilage-cartilage ROI.

In early stance, the WCoC on both medial and lateral plateaus first moved anteriorly reaching a maximum velocity of 26.7 mm/sec for the medial plateau and 77.7 mm/sec for the lateral plateau at 2.5% of the gait cycle. WCoC then moved posteriorly until 14% of the gait cycle with a maximum velocity of 106.5 mm/sec and 44.0 mm/sec for the medial and lateral plateaus respectively (Figure 6A black lines). At 14% of gait the medial WCoC moved in an anterior direction and the lateral WCoC moved in a posterior direction, suggesting that the primary motion of the tibia is in rotation. The rotation of the WCoC (Figure 6A grey dotted line) during the stance phase of walking first rotated externally until 14% of the gait cycle, then rotated internally before rotating externally again between 50% and 60% of the cycle. During stair climbing, all knees had an anterior shift of the WCoC on the medial plateau and a posterior shift of the WCoC on the lateral plateau at 20% to 40% of the cycle leading to an external rotation of the WCoC between 20% and 40% of the stair climb cycle (Figure 6B). Between 40% and 60% of stair climb the WCoC on the medial and lateral plateau remained in a fixed position; neither translating nor rotating. After 60% of stair climb the WCoC could not be consistently calculated due to the small axial loads being applied.

Discussion

By way of a novel experimental model that mimics gait and stair climb, we have fully quantified the dynamic contact mechanics of the human knee. Our data indicates that the magnitude of contact stress experienced by articular cartilage is highly dependent on its location on the tibial plateau and the activity being modeled. Specifically, during gait, peak contact stresses on the medial plateau occurred in areas of cartilage-cartilage contact; while during stair climb, peak contact stresses were located in the posterior aspect of the plateau, under the meniscus. On the lateral plateau, during gait and in early stair-climb, peak contact stresses occurred under the meniscus, while late in the stance phase of stair-climb, peak contact stresses were experienced in the zone of cartilage-cartilage contact. Furthermore, at 45% of the gait cycle, and at 20% and 48% of the stair climb cycle, peak stresses were simultaneously experienced on both the medial and lateral compartment, suggesting that these phases of loading warrant particular consideration in any simulation intended to evaluate scaffold performance. Finally, contact on the tibial plateau moved in a predictable manner, based on tibial kinematics, reaching peak velocities of 107 mm/s on the medial plateau during gait. Our study suggests that in order to design a scaffold capable of restoring ‘normal’ contact mechanics to the injured knees, the mechanics of the intended site of implantation should be taken into account in any pre-clinical testing regime.

The simulator has been previously used to analyze the effect of meniscal and ligament injury on knee joint contact mechanics at specific points in the walking cycle (Bedi et al. 2010, 2012, 2013). However a thorough analysis of contact mechanics *throughout* gait was not previously possible and stair climb has not been analyzed. To provide confidence in the ability of our force controlled simulator to result in physiological kinematics, we analyzed the translations and rotations of the tibia relative to the femur throughout gait and stair-climb and compared it to that presented in literature. During gait, the posterior translation and external rotation of the tibia that occurred at heel strike in our model fall within the magnitude and directions reported by (Andriacchi and Dyrby, 2005; Lafortune et al., 1992).

Furthermore, the change in direction of tibial translation which occurred at 5% of gait when an anterior translation commenced, followed the same pattern of magnitude and direction to that reported by (Kozanek et al., 2009; Lafortune et al., 1992). From 5% to almost 90% of the gait cycle, the tibiae in our model remained in an anterior location, with a peak anterior position occurring at approximately 70% of the gait cycle. The rather stable location of the tibia in an anterior location has also been reported clinically (Andriacchi and Dyrby, 2005; Kozanek et al., 2009; Lafortune et al., 1992); however (Kozanek et al., 2009), (Lafortune et al., 1992), and (Koo and Andriacchi, 2008), reported a posterior translation towards the end of the stance phase that was not mimicked in our study. The magnitude and direction of medial-lateral translation and varus-valgus rotation were also similar to that reported by (Kozanek et al., 2009; Lafortune et al., 1992). While substantial data on knee kinematics is available for the activity of walking, much less data is available on how the tibia moves relative to the femur during stair-climb.(Goyal et al., 2012) reported external rotations of the tibia from 20–60 % of the cycle, followed by internal rotation for the remainder of the cycle. While these directions mirror that reported in our study, the magnitude of rotation that we report (25–30°) was significantly less than that reported by (Goyal et al., 2012), 5–15°. Data reported by (Gao et al., 2012), and (Costigan et al., 2002), also suggested that the magnitude of tibial rotation during stair-climb is low (5–10º); but contrary to that reported by Goyal et al., their tibiae only demonstrated appreciable rotations after 60% of the cycle (Gao et al., 2012). In summary, knee kinematics reported in this study are within the envelope of that reported in literature.

During gait, there were no differences in the contact area between the medial and lateral plateaus but there was a difference in the maximum stress at 14% of gait, with the lateral plateau experiencing higher *peak* contact stresses. At this point of the gait cycle, the loads on the medial plateau were distributed evenly between the meniscal-cartilage and cartilage-cartilage ROIs. At the second axial peak (45% of gait), the ratio of load is shifted to areas of cartilage-cartilage contact. This result suggests that the medial meniscus plays a dominant load carrying role during the early phase of stance, and less so during the latter portions of stance; further suggesting that pre-clinical tests intended to evaluate the functional performance of scaffolds for medial meniscal repair should mimic early stance. On the lateral plateau, however, loads are distributed equally between the cartilage and the meniscus throughout gait, suggesting that the lateral meniscus functions to carry load throughout gait. When the knees were subjected to stair climb, peak contact stresses occurred in both compartments at 20% and 48% of the cycle; with stresses highest on the posterior aspect of the medial plateau under the meniscus. The variation in loads between cartilage-cartilage and meniscal-cartilage ROIs, are in line with regional variations in cartilage thickness (Li et al., 2005) and mechanical properties (Deneweth et al., 2013) that have previously been reported for human knees. Taken together, this information suggest that scaffolds for the repair of cartilage defects, should not only have different geometric requirements depending on their location in the knee joint, but also different load bearing requirements.

The WCoC parameter was developed to allow us to track contact on the tibia throughout both activities. As described previously for gait (Koo and Andriacchi, 2008; Kozanek et al.,

2009), contact on the tibial plateau first moves posteriorly then anteriorly in early stance before rotating internally in mid-to-late stance. The WCoC motions measured in our study, mimic these motions, and correlate with the AP translations and IE rotations of the tibia of the knees tested in this study during different phases of gait (see supplement). The motion of the WCoC on the medial and lateral plateaus during gait suggests a pivot about the lateral compartment which is similar to that recently described by (Kozanek et al., 2009) and (Koo and Andriacchi, 2008). During the stance phase of stair climbing there was very little movement of the WCoC. The correlation between the kinematic velocities and the IE WCoC velocities were high (see supplement) and suggest a medial pivot around which the lateral WCoC swings, which has been previously reported for quasi-static activities such as lunging and squatting (Li et al., 2005; Wunschel et al., 2011).

Increased velocity of contact between the tibia and femur has been correlated with increased rates of articular cartilage degeneration in an ovine model (Beveridge et al., 2013); suggesting that scaffolds to repair ligamentous soft tissue injuries should result in velocities of contact that do not differ significantly from that of the intact knee so as to avoid further cartilage injury. Despite this requirement, no data exists that describes the velocity of directly measured contact in human knees during activities of daily living. We have demonstrated that during early stance, the velocities of the WCoC alternated from anterior to posterior, with peak values of 77.7 mm/sec and 106.5 mm/sec for the anterior and posterior motions respectively. These high velocities are most likely caused by the rapid changes in the applied AP forces associated with heel strike and weight acceptance phases of stance when the muscles are activated to stabilize the joint after swing up to 14% of the gait cycle. For the activity of stair climb, maximum external rotational velocity of 22.3 °/sec was computed. The significance of these values lies in the fact that any cartilage or meniscal substitute should be able to structurally withstand physiological contact velocities. It might also be possible to pre-condition scaffolds for articular cartilage repair under conditions that mimic migratory contact profiles in order to harness the innate ability of the cells to respond to multi-directional stresses in vitro (Chen et al., 2012).

This study has several limitations. The sample size was small, and the full stair-climb cycle could not be simulated. While the knee kinematics as measured in this study mimicked that seen in gait analysis studies, during the later portions of the walking cycle there was no difference in the maximum stress seen on the two plateaus. This finding is contrary to those reported in literature (Yang et al., 2010) and may be caused by our inability to control varus-valgus moments (Andriacchi, 1994).

In summary, using an experimental model of the knee joint, we have fully quantified the dynamic contact mechanics on the tibial plateau during gait and stair climb. We suggest that scaffolds intended to treat cartilage or meniscal defects should be mechanically evaluated under conditions that take into account the contact mechanics in the intended location. Only then can be sure that a candidate scaffold will function appropriately in the highly loaded environment of the knee.

Supplementary Material

Refer to Web version on PubMed Central for supplementary material.

Acknowledgments

Research reported in this publication was supported by the National Institute of Arthritis and Musculoskeletal and Skin Diseases, part of the National Institutes of Health, under Award Numbers R01AR057343, T32-AR007281-27, and AR057343. The content is solely the responsibility of the authors and does not necessarily represent the official views of the National Institutes of Health. We thank the Clark & Kirby Foundations and the Russell Warren Chair in Tissue Engineering. We thank Carl Imhauser for assistance with the design of the fixtures.

References

Andriacchi TP. Dynamics of knee malalignment. The Orthopedic clinics of North America. 1994; 25:395–403. [PubMed: 8028883]

Andriacchi TP, Dyrby CO. Interactions between kinematics and loading during walking for the normal and ACL deficient knee. Journal of biomechanics. 2005; 38:293–298. [PubMed: 15598456]

AufderHeide AC, Athanasiou KA. Mechanical stimulation toward tissue engineering of the knee meniscus. Annals of biomedical engineering. 2004; 32:1161–1174. [PubMed: 15446512]

Bedi A, Kelly NH, Baad M, Fox AJ, Brophy RH, Warren RF, Maher SA. Dynamic contact mechanics of the medial meniscus as a function of radial tear, repair, and partial meniscectomy. The Journal of bone and joint surgery. American volume. 2010; 92:1398–1408.

Beveridge JE, Heard BJ, Shrive NG, Frank CB. Tibiofemoral centroid velocity correlates more consistently with Cartilage damage than does contact path length in two ovine models of stifle injury. Journal of orthopaedic research : official publication of the Orthopaedic Research Society. 2013

Brimacombe JM, Wilson DR, Hodgson AJ, Ho KC, Anglin C. Effect of calibration method on Tekscan sensor accuracy. Journal of biomechanical engineering. 2009; 131:034503. [PubMed: 19154074]

Chen T, Buckley M, Cohen I, Bonassar L, Awad HA. Insights into interstitial flow, shear stress, and mass transport effects on ECM heterogeneity in bioreactor-cultivated engineered cartilage hydrogels. Biomechanics and modeling in mechanobiology. 2012; 11:689–702. [PubMed: 21853351]

Costigan PA, Deluzio KJ, Wyss UP. Knee and hip kinetics during normal stair climbing. Gait & posture. 2002; 16:31–37. [PubMed: 12127184]

Deneweth JM, Newman KE, Sylvia SM, McLean SG, Arruda EM. Heterogeneity of tibial plateau cartilage in response to a physiological compressive strain rate. Journal of orthopaedic research : official publication of the Orthopaedic Research Society. 2013; 31:370–375. [PubMed: 22952052]

Dyrby CO, Andriacchi TP. Secondary motions of the knee during weight bearing and non-weight bearing activities. Journal of orthopaedic research : official publication of the Orthopaedic Research Society. 2004; 22:794–800. [PubMed: 15183436]

Fornalski S, McGarry MH, Bui CN, Kim WC, Lee TQ. Biomechanical effects of joint line elevation in total knee arthroplasty. Clinical biomechanics. 2012; 27:824–829. [PubMed: 22727620]

Freed LE, Guilak F, Guo XE, Gray ML, Tranquillo R, Holmes JW, Radisic M, Sefton MV, Kaplan D, Vunjak-Novakovic G. Advanced tools for tissue engineering: scaffolds, bioreactors, and signaling. Tissue engineering. 2006; 12:3285–3305. [PubMed: 17518670]

Gao B, Cordova ML, Zheng NN. Three-dimensional joint kinematics of ACL-deficient and ACL-reconstructed knees during stair ascent and descent. Human movement science. 2012; 31:222–235. [PubMed: 21798608]

Goyal K, Tashman S, Wang JH, Li K, Zhang X, Harner C. In vivo analysis of the isolated posterior cruciate ligament-deficient knee during functional activities. The American journal of sports medicine. 2012; 40:777–785. [PubMed: 22328708]

Grood ES, Suntay WJ. A joint coordinate system for the clinical description of three-dimensional motions: application to the knee. Journal of biomechanical engineering. 1983; 105:136–144. [PubMed: 6865355]

Hopkins AR, New AM, Rodriguez-y-Baena F, Taylor M. Finite element analysis of unicompartmental knee arthroplasty. Medical engineering & physics. 2010; 32:14–21. [PubMed: 19897397]

Koo S, Andriacchi TP. The knee joint center of rotation is predominantly on the lateral side during normal walking. Journal of biomechanics. 2008; 41:1269–1273. [PubMed: 18313060]

Kozanek M, Hosseini A, Liu F, Van de Velde SK, Gill TJ, Rubash HE, Li G. Tibiofemoral kinematics and condylar motion during the stance phase of gait. Journal of biomechanics. 2009; 42:1877–1884. [PubMed: 19497573]

Lafortune MA, Cavanagh PR, Sommer HJ 3rd, Kalenak A. Three-dimensional kinematics of the human knee during walking. Journal of biomechanics. 1992; 25:347–357. [PubMed: 1583014]

Li G, Most E, Sultan PG, Schule S, Zayontz S, Park SE, Rubash HE. Knee kinematics with a high-flexion posterior stabilized total knee prosthesis: an in vitro robotic experimental investigation. The Journal of bone and joint surgery. 2004; 86-A:1721–1729. American volume. [PubMed: 15292421]

Li G, Park SE, DeFrate LE, Schutzer ME, Ji L, Gill TJ, Rubash HE. The cartilage thickness distribution in the tibiofemoral joint and its correlation with cartilage-to-cartilage contact. Clinical biomechanics. 2005; 20:736–744. [PubMed: 15963613]

Mononen ME, Jurvelin JS, Korhonen RK. Effects of radial tears and partial meniscectomy of lateral meniscus on the knee joint mechanics during the stance phase of the gait cycle-A 3D finite element study. Journal of orthopaedic research : official publication of the Orthopaedic Research Society. 2013; 31:1208–1217. [PubMed: 23572353]

Mundermann A, Dyrby CO, D'Lima DD, Colwell CW Jr, Andriacchi TP. In vivo knee loading characteristics during activities of daily living as measured by an instrumented total knee replacement. Journal of orthopaedic research : official publication of the Orthopaedic Research Society. 2008; 26:1167–1172. [PubMed: 18404700]

Netravali NA, Koo S, Giori NJ, Andriacchi TP. The effect of kinematic and kinetic changes on meniscal strains during gait. Journal of biomechanical engineering. 2011; 133:011006. [PubMed: 21186896]

Scanlan SF, Chaudhari AM, Dyrby CO, Andriacchi TP. Differences in tibial rotation during walking in ACL reconstructed and healthy contralateral knees. Journal of biomechanics. 2010; 43:1817–1822. [PubMed: 20181339]

Seitz AM, Lubomierski A, Friemert B, Ignatius A, Durselen L. Effect of partial meniscectomy at the medial posterior horn on tibiofemoral contact mechanics and meniscal hoop strains in human knees. Journal of orthopaedic research : official publication of the Orthopaedic Research Society. 2012; 30:934–942. [PubMed: 22072570]

Taylor SJ, Perry JS, Meswania JM, Donaldson N, Walker PS, Cannon SR. Telemetry of forces from proximal femoral replacements and relevance to fixation. Journal of biomechanics. 1997; 30:225–234. [PubMed: 9119821]

Wunschel M, Leichtle U, Lo J, Wulker N, Muller O. Differences in tibiofemoral kinematics between the unloaded robotic passive path and a weightbearing knee simulator. Orthopedic reviews. 2012; 4:e2. [PubMed: 22577503]

Wunschel M, Leichtle U, Obloh C, Wulker N, Muller O. The effect of different quadriceps loading patterns on tibiofemoral joint kinematics and patellofemoral contact pressure during simulated partial weight-bearing knee flexion. Knee surgery, sports traumatology, arthroscopy : official journal of the ESSKA. 2011; 19:1099–1106.

Yang NH, Canavan PK, Nayeb-Hashemi H, Najafi B, Vaziri A. Protocol for constructing subject-specific biomechanical models of knee joint. Computer methods in biomechanics and biomedical engineering. 2010; 13:589–603. [PubMed: 20521186]

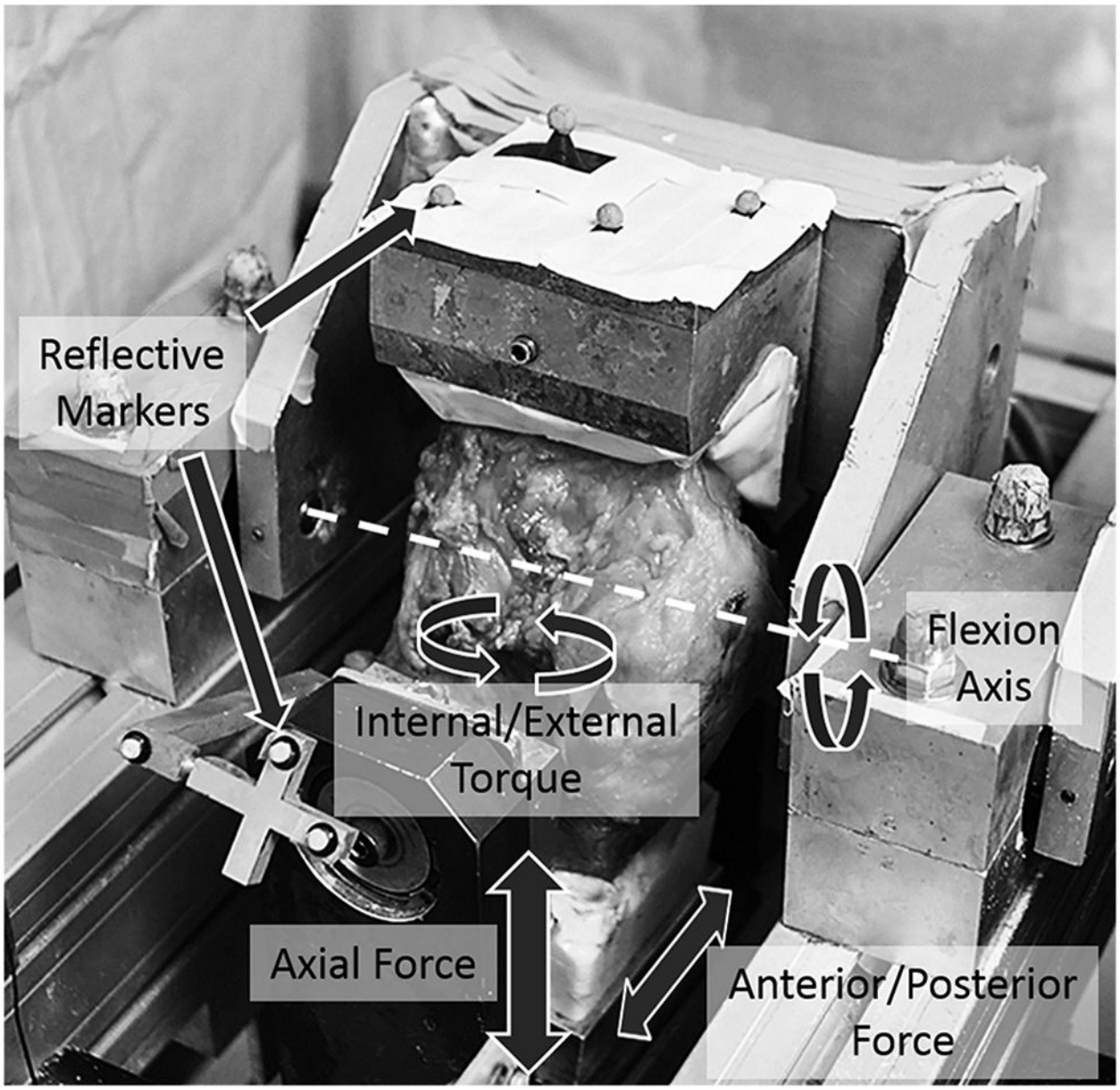

Figure 1. Dynamic gait simulator

Image of cadaveric knee on the Stanmore knee simulator. The simulator applies axial force, anterior/posterior force, internal/external torque and flexion/extension rotation the motion of which can be measure using reflective markers attached to the femur and tibia pots.

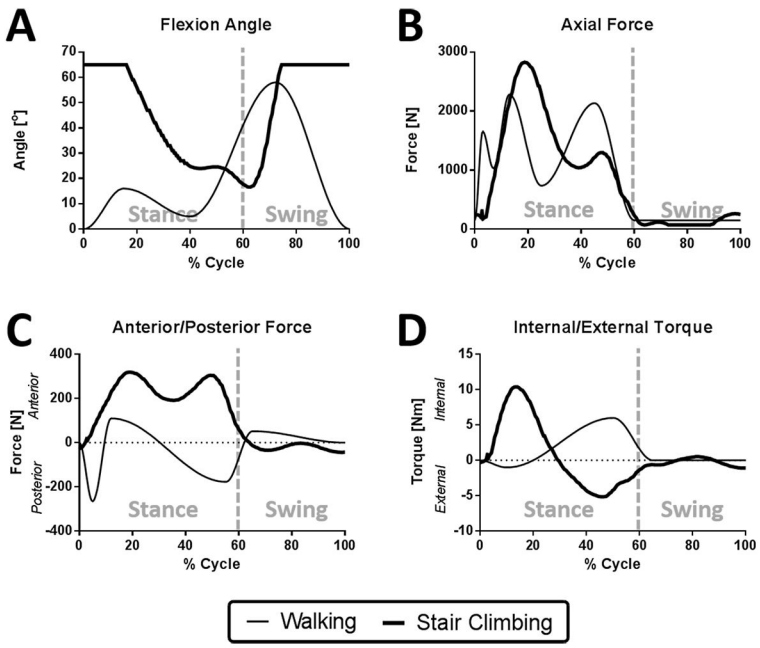

Figure 2. Dynamic simulator inputs for walking and stair climbing

Inputs for A) flexion angle, B) axial force, C) anterior/posterior force, and D) internal/external torque were applied to the cadaveric knees. Note that the flexion angle for stair climbing is truncated above 65° due to the limitations of the simulator.

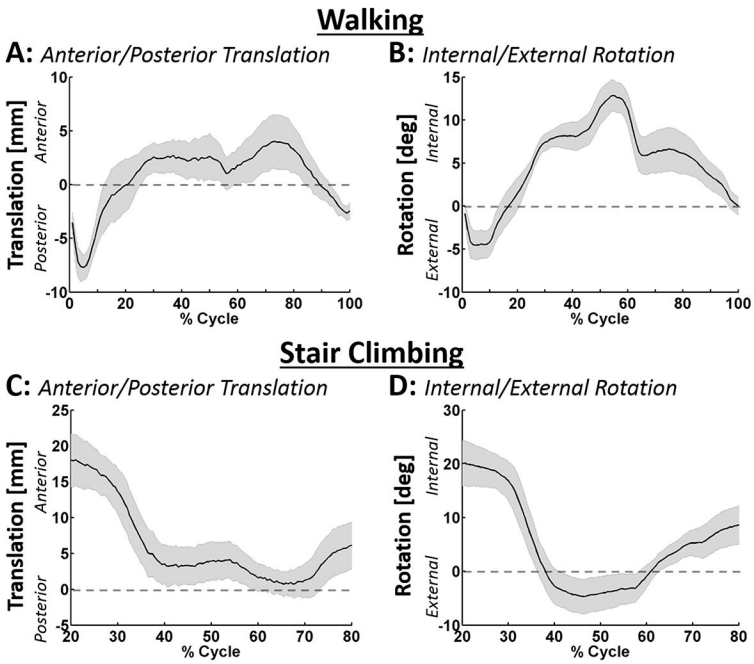

Figure 3. Measured kinematic AP translations and IE rotations during walking and stair climbing

The average AP translation and IE rotation for A&B) walking and C&D) stair climbing were calculated using the kinematic markers placed on the femur and tibia pots. The black lines represent the mean and the shaded regions represent the standard error for the five knees tested.

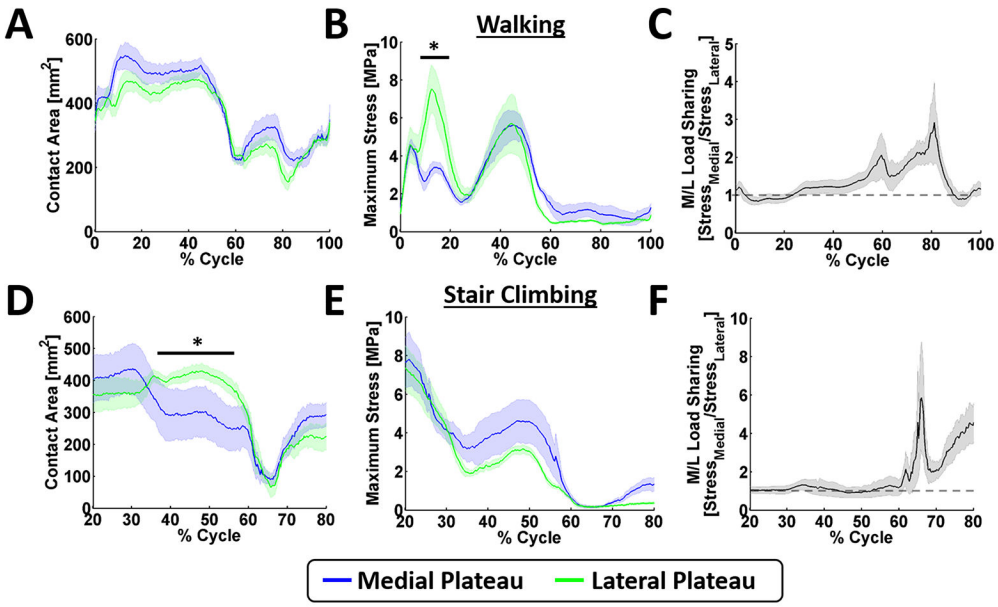

Figure 4. Average contact area and stress during walking and stair climbing

The A&D) contact area, B&E) maximum stress, and C&F) medial/lateral load sharing for walking and stair climbing were calculated using the normal stress measurements collected from the electronic sensors. The data is represented as the mean and standard error. The dotted line in C & F represent equal sharing between the medial and lateral plateaus. * denotes $p < 0.05$.

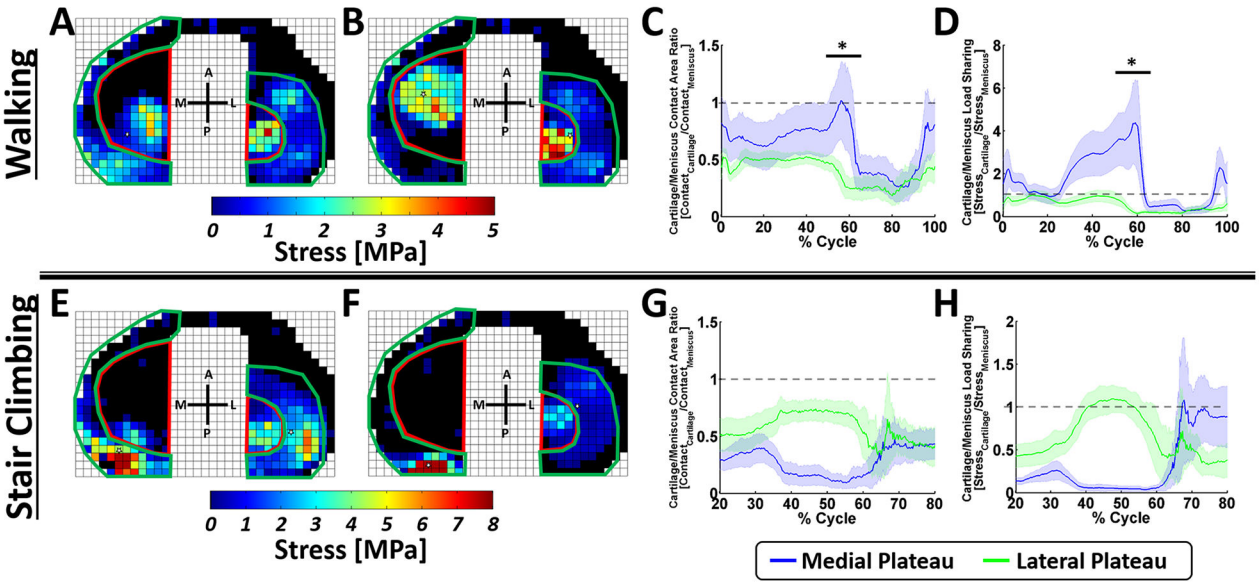

Figure 5. Cartilage-to-meniscal ratios for contact area and stress

For walking, the cartilage-cartilage contact area (red) were outlined, using A) 14% and B) 45% of the gait cycle as reference, such that the cartilage-cartilage contact fell within the region of interest throughout the gait cycle, the remainder of the plateau was taken as the meniscal-cartilage contact region (green). The ratios between the cartilage and meniscal C) contact area and D) load sharing were then calculated using these regions. The same cartilage-cartilage and meniscal-cartilage regions were used for stair climbing [shown here for E) 19% and F) 48% of the stair climb cycle] and the ratios between the cartilage and meniscal G) contact area and H) load sharing were measured. * denotes $p < 0.05$.

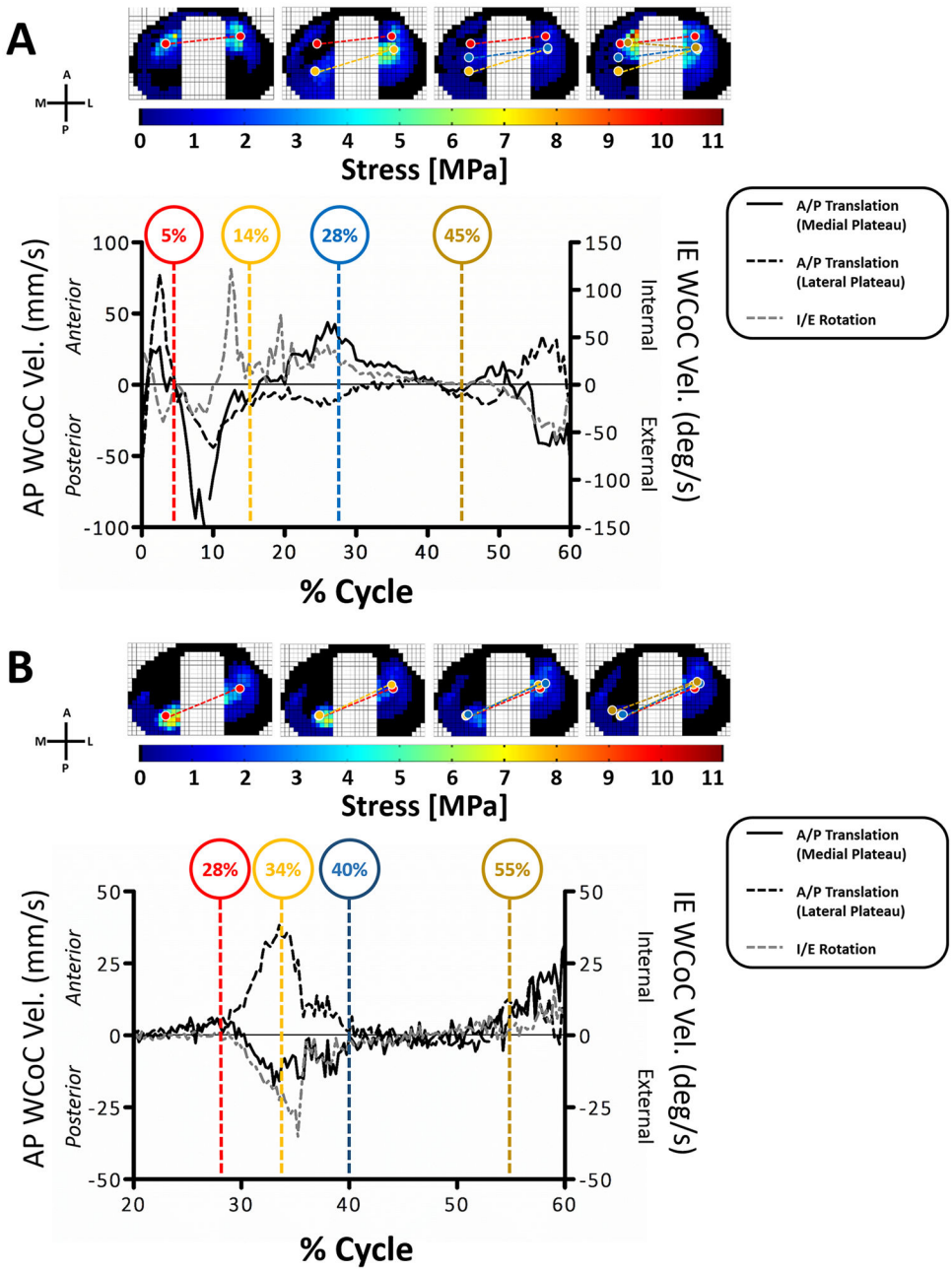

Figure 6. The weighted center of contact AP and IE velocities

The average WCoC velocity during A) walking and B) stair climbing for all knees are shown in the graphs. The upper images show the stress magnitudes and WCoC locations on the medial and lateral plateaus (circles) for a representative knee. The color of the WCoC circles corresponds to the colors of the % cycle highlighted in the graphs.